JOURNAL OF COMPUTATIONAL PHYSICS 66, 469–480 (1986)

An Orbit-Averaged Darwin Quasi-neutral Hybrid Code

ANDREW L. ZACHARY

Institute of Geophysics and Planetary Physics,
Lawrence Livermore National Laboratory, Livermore, California 94550

AND

BRUCE I. COHEN

Lawrence Livermore National Laboratory, Livermore, California 94550

Received September 27, 1985; revised January 16, 1986

DEDICATED TO THE MEMORY OF RAYMOND C. GRIMM

We have developed an orbit-averaged Darwin quasi-neutral hybrid code to study the *in situ* acceleration of cosmic ray by supernova-remnant shock waves. The orbit-averaged algorithm is well suited to following the slow growth of Alfvén waves driven by resonances with rapidly gyrating cosmic rays. We present a complete description of our algorithm, along with stability and noise analyses. The code is numerically unstable, but a single *e*-folding may require as many as 10^5 time-steps! It can therefore be used to study instabilities for which $\Gamma_{\text{physical}} > \Gamma_{\text{numerical}}$, provided that $\Gamma_{\text{numerical}} \tau^{\text{final}} < O(1)$. We also analyze a physical instability which provides a successful test of our algorithm.

1. INTRODUCTION

We have developed an orbit-averaged Darwin quasi-neutral hybrid code to study the *in situ* acceleration of cosmic ray ions by supernova-remnant shock waves. In current models of this acceleration [1–4], suprathermal particles gain energy as they bounce back and forth across the shock. Turbulence behind the shock provides the downstream scattering centers, while upstream, the particles which stream ahead of the shock generate resonant Alfvén waves, and in turn are pitch-angle scattered by them. The low-temperature ions in the interstellar medium provide the inertia for the waves, with the energy for the instability coming from the streaming of the low-density relativistic cosmic rays. These models are attractive because they can account for the galactic cosmic ray energy density and because they naturally reproduce the observed shape of the cosmic ray energy spectrum.

Despite its attractions, supernova-remnant acceleration has two serious problems. First, supernova remnants have a finite lifetime, so the cosmic ray spec-

0021-9991/86 $3.00

trum will have a maximum energy. Recent work [5] suggests a firm upper limit of $E_{max} \leqslant 10^{15}$ eV, but observations show a smooth spectrum up to at least 10^{20} eV. Second, near the shock front, the turbulent energy generated by the streaming particles violates the quasi-linear assumption $\delta B/B \ll 1$. The entire picture of pitch-angle scattering by resonant waves given by weak turbulence theory then needs substantial modification.

Our code has been developed to study the region ahead of a supernova shock, where the mildly relativistic ions which make up the bulk of the galactic cosmic rays interact with Alfvén wave turbulence. The cosmic rays and interstellar material have similar energy densities, but the interstellar ions are 10^{5-7} times as abundant. We therefore represent the electrons and ions in the interstellar medium by a set of one-dimensional single-fluid MHD equations, while the energetic cosmic ray ions are treated as kinetic particles. The cosmic ray current and density are included in the MHD equations as source terms. A nonrelativistic treatment of the MHD fluid accurately describes the interactions between the cosmic ray ions and the fluid because pitch angle scattering forces the bulk velocity of the cosmic rays to be close to the Alfvén velocity. The MHD equations are solved explicitly with no penalty on the time-step to resolve the Alfvén wave frequency. Furthermore, because the frequencies and growth rates of the Alfvén waves are typically orders of magnitude smaller than the cyclotron frequency of the resonant cosmic rays, we have orbit-averaged [6] the cosmic ray source terms in the MHD equations.

We outline our method of solution of the coupled MHD-particle equations (Sect. 2), present a linear stability analysis for our code, including both finite Δx and finite ΔT terms (Sect. 3), discuss some practical considerations in implementing the code (Sect. 4), and give some examples. In previous work [7], an explicit predictor–corrector magneto-inductive code was shown to be stable at large time-step. We shall show that our algorithm is unstable at all time-steps, but with the proper choice of operating parameters, the numerical instability can require as many as 10^6 time-steps for a single e-folding and does not interfere with the study of physical problems of interest.

2. Description of the Algorithm

Our physical system has three species: low temperature, high density interstellar electrons and ions; and mildly relativistic, low density cosmic ray ions. The interstellar material is represented by a set of one-dimensional, single fluid MHD equations, which is advanced on the macro-time scale ΔT. The particles are advanced on the much more rapid micro-time scale Δt ($\equiv \Delta T/N$). In Fig. 1, we show the sequence of operations for the relative advance of the fields and particles. With given fields, we advance the particle positions and velocities through N micro time-steps using the relativistic mover described in [8]. To advance the MHD equations

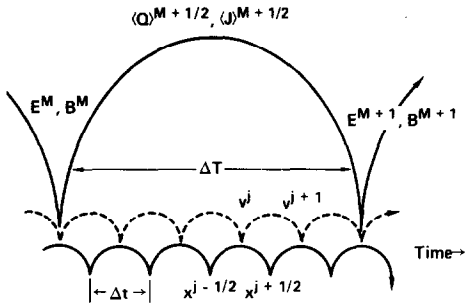

FIG. 1. The application of orbit-averaging to the time-advance of the field and particle equations. The particles are advanced on the short time scale Δt, during which the orbit-averaged souce terms $\langle Q \rangle$ and $\langle \mathbf{j} \rangle$ are accumulated. The fields are then advanced on the much longer time scale ΔT. For clarity, the fluid variables ρ, P, and $\mathbf{u}$, which are advanced along with $\mathbf{E}$ and $\mathbf{B}$, are omitted from the diagram.

with particle source terms, we construct the orbit-averaged charge density and current as

$$\langle Q \rangle^{M+(1/2)} = \frac{1}{N+1} \sum_{l=0}^{N} q n^{l\Delta t}, \tag{1}$$

$$\langle \mathbf{j} \rangle^{M+(1/2)} = \frac{1}{N+1} \sum_{l=0}^{N} q n^{l\Delta t} \mathbf{v}^{l\Delta t}, \tag{2}$$

where $n^{l\Delta t}$ and $\mathbf{v}^{l\Delta t}$ are the grid-interpolated mean number density and velocity of the cosmic rays at time $t = l\,\Delta t$.

With these definitions and the quasi-neutrality condition $n_e = n_i + n_{cr}$, where $n_{cr} \equiv$ cosmic ray number density, we can write down a set of single-fluid MHD equations which represent the response of the fields and interstellar material to the cosmic rays. In the limit $n_{cr}/n_i \ll 1$, these equations are

$$\frac{\partial \rho}{\partial t} + \frac{\partial}{\partial x}(\rho u_x) = 0, \tag{3}$$

$$\frac{\partial}{\partial t}(\rho u_j) + \frac{\partial}{\partial x}\left\{ P\delta_{jx} + \rho u_j u_x - \frac{B_x B_j}{4\pi} + \frac{B^2}{4\pi}\delta_{jx} \right\} = -\langle Q \rangle_{cr} E_j - \frac{(\langle \mathbf{j} \rangle_{cr} \times \mathbf{B})_j}{c} \tag{4}$$

$$\frac{\partial}{\partial t}\left\{ \frac{P}{\gamma - 1} + \frac{1}{2}\rho u^2 + \frac{B^2}{8\pi} \right\} + \frac{\partial}{\partial x}\left\{ \left(\frac{\gamma}{\gamma - 1} P + \frac{1}{2}\rho u^2 \right) u_x + B_y (\mathbf{u} \times \mathbf{B})_z - B_z (\mathbf{u} \times \mathbf{B})_y \right\} = -\langle j \rangle_{cr} \cdot \mathbf{E}, \tag{5}$$

$$\frac{\partial \mathbf{B}}{\partial t} + \frac{\partial}{\partial x}\{(\mathbf{u} \times \mathbf{B}) \times \hat{\mathbf{x}}\} = 0, \tag{6}$$

$$\mathbf{E} = -\frac{\mathbf{u} \times \mathbf{B}}{c}, \tag{7}$$

where $\langle \mathbf{j} \rangle_{cr}$ and $\langle Q \rangle_{cr}$ are the orbit averaged current and density, $\mathbf{u}$ is the bulk fluid velocity, P is the fluid pressure, and γ is the adiabatic index.

Each of these equations has the form

$$\frac{\partial u}{\partial t} + \frac{\partial}{\partial x} F(u) = S, \tag{8}$$

where F is an arbitrary function of u, and S is independent of u. We use a modified Lax–Wendroff scheme, known as MacCormack's method, to solve the coupled equations. Expicitly, we have

$$\tilde{u}_i^{n+1} = u_i^n - \frac{\Delta T}{\Delta x}(F_{i+1}^n - F_i^n) + \frac{\Delta T}{2}(S_{i+1}^{n+(1/2)} + S_i^{n+(1/2)}), \tag{9a}$$

$$u_i^{n+1} = \frac{1}{2}(\tilde{u}_i^{n+1} + u_i^n) - \frac{\Delta T}{2\Delta x}(\tilde{F}_i^{n+1} - \tilde{F}_{i-1}^{n+1}) + \frac{\Delta T}{4}(S_i^{n+(1/2)} + S_{i-1}^{n+(1/2)}). \tag{9b}$$

MacCormack's method is of second order in Δx and ΔT, and is subject to the usual Courant stability condition

$$c\frac{\Delta T}{\Delta x} \leqslant 1,$$

where c is a characteristic speed [9]. We have added an artificial viscosity to prevent the possible formation of unresolved shocks.

The time advance of the systems as a whole must be carefully constructed to make certain all quantities are known at the correct time level. Suppose that we know the MHD variables ρ, P, $\mathbf{u}$, $\mathbf{B}$, and $\mathbf{E}$ at time $M\Delta T$, and that the particle velocities are at time $M\Delta T$, with positions at time $(M\Delta T + \Delta t/2)$. The orbit-averaged current and charge density are then at time $(M - \frac{1}{2})\Delta T$.

Each advance to the next time level begins with a half-advance of the fluid to time $(M + \frac{1}{2})\Delta T$. The intermediate fields $\mathbf{E}^{M+(1/2)}$, $\mathbf{B}^{M+(1/2)}$ advance the particles a full macro time-step to $M\Delta T$, and along the way, we accumulate the orbit-averaged current and density. Finally, these new orbit-averaged quantities are used to construct source terms at time $(M + \frac{1}{2})\Delta T$, and the fields are advanced a full time-step from $M\Delta T$ to $(M+1)\Delta T$. In Fig. 2, we show the timing for the advance of the system as a whole. This scheme is second-order accurate in ΔT and requires that the particles be advanced only once from $M\Delta T$ to $(M+1)\Delta T$, rather than twice as in the predictor–corrector scheme described in [6]. We speculate that the weak numerical instability present in our method may arise from this single advance of

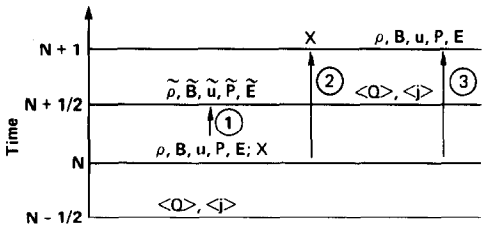

FIG. 2. The details of the three stage time advance of the coupled MHD-particle equations. The $\langle Q \rangle$ and $\langle \mathbf{j} \rangle$ at time level $N-(1/2)$, along with ρ, $\mathbf{B}$, $\mathbf{u}$, P, and $\mathbf{E}$ at time level N are used to construct the temporary results $\tilde{\rho}$, $\tilde{\mathbf{B}}$, $\tilde{\mathbf{u}}$, $\tilde{P}$, and $\tilde{\mathbf{E}}$ at time level $N+(1/2)$. The fields $\tilde{\mathbf{E}}$ and $\tilde{\mathbf{B}}$ advance the particles to time $N+1$. Finally, $\langle Q \rangle$ and $\langle \mathbf{j} \rangle$ at time $N+(1/2)$ advance the MHD variables from time level N to $N+1$.

the particles. In exchange for this instability, we gain a factor of 2 in speed, and a similar improvement in computer memory requirements.

Our unconventional choice for the particle time levels, with the velocity known on the time-step, and the position on the half-time-step, was done to ensure that in the limit $\Delta T \to \Delta t$, $\langle \mathbf{j} \rangle$ and $\langle Q \rangle$ go over to their nonorbit-averaged counterparts. We have taken similar care in the initialization of the particle positions and velocities.

3. Linear Stability Analysis

The linear stability analysis breaks in a natural way into three parts. In the first part, we discuss the conditions on the stability of the fluid algorithm in the absence of particles. As expected for a simple advective scheme, MacCormack's method is highly diffusive and dispersive. In the next part, we reanalyze the linear equations of motion derived in [7], and reduce Eqs. (9)–(11) in [7] to a more tractable form involving rotation matrices which describe the orbit-averaging. Finally, we discuss the stability of the algorithm for fluid and particles presented above.

The finite Δx, ΔT von Neumann stability analysis of Eqs. (3)–(7) with no discrete particle source terms is straightforward. After some algebra, we find $\mathrm{Re}(\omega\,\Delta T)$ and $\mathrm{Im}(\omega\,\Delta T)$ to be

$$\mathrm{Re}(\omega\,\Delta T) = \tan^{-1}\left\{\frac{\pm(v_A \Delta T/\Delta x)\sin(k\,\Delta x)}{1-2(v_A^2\,\Delta T^2/\Delta x^2)\sin^2(k\,\Delta x/2)}\right\}, \tag{10}$$

$$\mathrm{Im}(\omega\,\Delta T) = \frac{1}{2}\log\left\{\left(1-\frac{2v_A^2\,\Delta T^2}{\Delta x^2}\sin^2\left(\frac{k\,\Delta x}{2}\right)\right)^2 + \frac{v_A^2\,\Delta T^2}{\Delta x^2}\sin^2(k\,\Delta x)\right\}, \tag{11}$$

where

$$v_A = \left(\frac{B_0^2}{4\pi\rho}\right)^{1/2} \equiv \text{Alfvén velocity.}$$

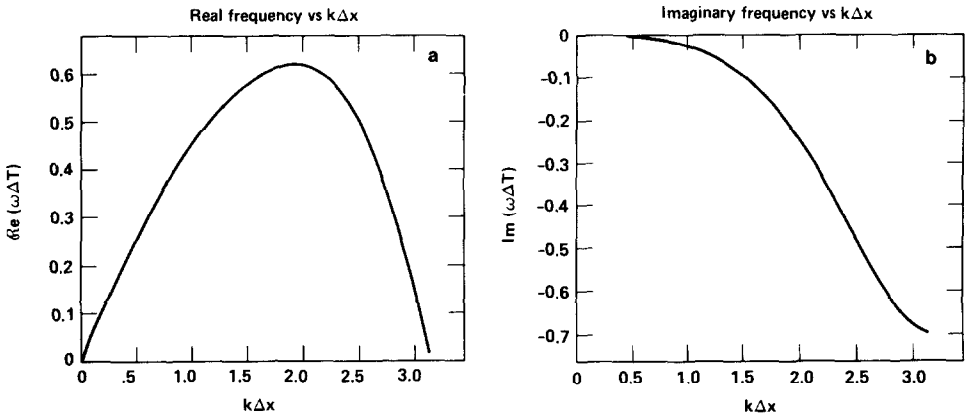

FIG. 3. The real and imaginary parts of the solutions of the dispersion relation for MacCormack's method. In both cases, we have used a Courant number of (1/2).

We show $\mathrm{Re}(\omega\,\Delta T)$ and $\mathrm{Im}(\omega\,\Delta T)$ as functions of $k\,\Delta x$ in Fig. 3. This analysis shows MacCormack's method to be stable if we satisfy the Courant condition

$$v_A \frac{\Delta T}{\Delta x} \leqslant 1.$$

A Taylor series expansion of the linearized MHD equations, as in Hirt's stability analysis [10], also shows MacCormack's method is stable whenever the Courant condition is satisfied.

We have extended the stability analysis of the orbit-averaging algorithm given in [7] by simplifying the matrix algebra involved in the particle rotation. The matrix operators in their Eqs. (9)–(11) are replaced by a single set of rotation matrices. The angle of rotation will be shown to be a multiple of an angle which naturally occurs in the linearized $\mathbf{v}\times\mathbf{B}$ motion. We assume that cold, uniformly distributed particles are immersed in a uniform magnetic field $\mathbf{B}_0$. The particles are non-relativistic, and $\mathbf{B}_0$ lies along the simulation axis, x. In assessing the stability of the longest wavelength modes it is sufficent to describe the particles in the limit $k\,\Delta x \to 0$. The velocities at a time $l\,\Delta t$ after the beginning of a macro-time interval are related to the initial velocities by

$$\begin{aligned}\mathbf{v}^l &= \frac{\boldsymbol{\theta}^{2l}}{|\theta|^l}\cdot\mathbf{v}^0 + \sum_{j=1}^{l}\frac{\boldsymbol{\theta}^{2j+1}}{|\theta|^{j+1}}\cdot\frac{q\,\Delta t}{m}\,\mathbf{E}^{M+(1/2)} \\ &= \left(\mathbf{I}-\frac{\boldsymbol{\theta}^2}{|\theta|}\right)^{-1}\cdot\left(\mathbf{I}-\frac{\boldsymbol{\theta}^{2l}}{|\theta|^l}\right)\cdot\frac{\boldsymbol{\theta}}{|\theta|}\cdot\frac{q\,\Delta t E^{M+1/2}}{m}+\frac{\boldsymbol{\theta}^{2l}}{|\theta|^l}\cdot\mathbf{v}^0, \qquad (12)\end{aligned}$$

with

$$\boldsymbol{\theta} = \begin{pmatrix} 1 & \chi \\ -\chi & 1 \end{pmatrix},$$

where $\chi = \Omega_i \Delta t/2$, $\Omega_i = qB_0/mc$, and $|\theta| = \det \boldsymbol{\theta} = 1 + \chi^2$. The last equation was obtained by summing a geometric series. The matrix

$$\boldsymbol{\Psi} \equiv \frac{\boldsymbol{\theta}^2}{|\theta|} = \begin{pmatrix} \dfrac{1-\chi^2}{1+\chi^2} & \dfrac{2\chi}{1+\chi^2} \\ \dfrac{-2\chi}{1+\chi^2} & \dfrac{1-\chi^2}{1+\chi^2} \end{pmatrix} \equiv \begin{pmatrix} \cos\theta & \sin\theta \\ -\sin\theta & \cos\theta \end{pmatrix}$$

has the form of a rotation matrix, where the rotation angle is defined by

$$\theta = \tan^{-1}\left(\frac{2\chi}{1-\chi^2}\right).$$

We now define the symbol [;] to represent a rotation matrix, with [; the diagonal elements and ;] the off-diagonal element. The sign of ;] corresponds to the sign of the lower left element. In this notation,

$$\boldsymbol{\Psi} \equiv [\cos\theta; -\sin\theta].$$

The p-fold application of $\boldsymbol{\Psi}$ is equivalent to a single rotation through an angle $(p\theta)$ so that the equation for $\mathbf{v}^l$ now reduces to

$$\mathbf{v}^l = [\cos(l\theta); -\sin(l\theta)]\mathbf{v}^0 + \frac{c}{B_0}[\sin(l\theta); -(1-\cos(l\theta))]\,\mathbf{E}^{M+1/2}. \tag{13}$$

The orbit-averaged, linearized current is calculated similarly

$$\begin{aligned}\langle \mathbf{j} \rangle^{M+1/2} &= \frac{1}{N+1}\sum_{l=0}^{N} qn_0\mathbf{v}^l \\ &= \left(\mathbf{I} - \frac{\boldsymbol{\theta}^2}{|\theta|}\right)^{-1} \cdot \left(\mathbf{I} - \frac{\boldsymbol{\theta}^{2N+2}}{|\theta|^{N+1}}\right)\frac{qn_0\mathbf{v}^M}{N+1} \\ &\quad + \left(\mathbf{I} - \frac{\boldsymbol{\theta}^2}{|\theta|}\right)^{-1} \cdot \left\{\mathbf{I} - \frac{1}{N+1}\left(\mathbf{I} - \frac{\boldsymbol{\theta}^2}{|\theta|}\right)^{-1} \cdot \left(\mathbf{I} - \frac{\boldsymbol{\theta}^{2N+2}}{|\theta|^{N+1}}\right)\right\} \\ &\quad \cdot \frac{\boldsymbol{\theta}}{|\theta|} \cdot \frac{q^2\,\Delta t\, n_0 \mathbf{E}^{M+1/2}}{m} \\ &= [P; -Q]\mathbf{v}^M - \frac{c}{B}[Q; 1-P]\,\mathbf{E}^{M+(1/2)},\end{aligned} \tag{14a}$$

where

$$P = \frac{1}{S}\left(1 - \cos(S\theta) + \frac{\sin(S\theta)}{\chi}\right),$$
$$Q = \frac{1}{S}\left(\sin(S\theta) - \frac{1 - \cos(S\theta)}{\chi}\right), \tag{14b}$$
$$S = N + 1,$$

and where $\mathbf{v}^M$ is the velocity vector at time $t = M\,\Delta T$.

We can use Eq. (13) to relate $\mathbf{v}^{M+1}$ to $\mathbf{v}^M$ and $\mathbf{E}^{M+(1/2)}$ by taking $l = N \equiv \Delta T/\Delta t$. The complete system of coupled particle-fluid equations is then closed with Eqs. (3)–(7) and (14), which relate the perturbed fields and currents. As is obvious, there is considerable algebra involved in the analysis, but the use of rotation operators makes the derivation manageable.

The resulting dispersion relation is a 5th order polynomial in $z \equiv \exp(-i\omega\,\Delta T)$, characterized by the parameter $\chi_{cr} \equiv (n_{cr}/n_i)\cdot(\Omega_i\,\Delta T/2)$. In the limit $n_{cr} \to 0$ we analytically recover four modes, two of which are shear Alfvén waves which obey the dispersion relation for MacCormack's method. The other two modes are undamped cyclotron oscillations at frequency $\omega = \Omega_i$.

For finite n_{cr}, two of the five modes are again shear Alfvén waves, and two are cyclotron modes. The Alfvén waves are stable until the Courant condition is violated, and one of the cyclotron modes is always neutrally stable. The other cyclotron mode is slightly unstable for all ΔT. The final mode is a heavily damped

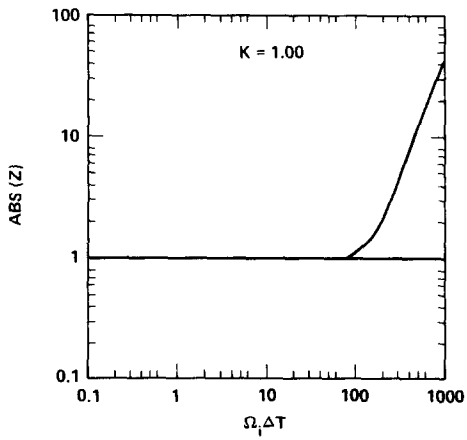

FIG. 4. The modulus of the amplification factor $z = \exp(-i\omega\,\Delta T)$ as a function of $\Omega_i\,\Delta T$ for the fundamental ($k = 1$) mode. In this example, $n_{cr}/n_i = 3.6 \times 10^{-5}$, $v_A = 10^{-2}$, $\Delta x = \pi/16$, and the orbit-averaging parameter $N = 50$. For $\Omega_i\,\Delta T < 20$, all the roots appear to be marginally stable, but one of the cyclotron roots is slightly unstable with $|z| - 1 \sim 10^{-5}$. When $\Omega_i\,\Delta T > 20$, the Alfven waves are unstable because the Courant condition is iolated. The heavily damped numerical mode is not plotted, typically it has $|z| < 10^{-7}$.

numerical mode which arises from the coupling of the fluid and particle equations. In Fig. 4, we present the solution of the combined dispersion relation for a typical case. In this example, the growth rate for numerical instability was $\leqslant 10^{-5}\,\Delta T^{-1}$ for $\Omega_i \Delta T \gg 1$ and proves to be no practical impediment to performing simulations. We again state that even though the code is formally unstable, we can still use it to study instabilities for which the growth rates Γ satisfy $\Gamma_{\text{physical}} \gg \Gamma_{\text{numerical}}$, provided that

$$\Gamma_{\text{numerical}} \tau^{\text{final}} < O(1).$$

4. Practical Considerations

In designing our code, we have paid particular attention to noise levels associated with discrete particle effects, and finite time step and Δx errors in the particle mover and field solver. Our physical growth rates are so small, $\Gamma < \omega \ll \Omega_i$, that any resonant instability may shut off well before saturation because of trapping in small amplitude noise fields [11]. Orbit-averaging can help reduce the noise amplitude associated with discrete particles effects. On the other hand, orbit-averaging requires some reinterpretation of the usual constraint $\Omega_i \Delta T \ll 1$ associated with most particle movers. As we shall show, the combination of small growth rates and orbit-averaging introduces several new constraint equations.

The statistical averaging performed in an orbit-averaged code can offer a large gain in computational efficiency. Each simulation particle samples a large volume of phase space during each macro-time-step, and the noise level inherent in the code is correspondingly reduced. With the use of some simple statistical arguments, we can derive the expected noise level for an initially uncorrelated distribution function.

If we make two reasonable assumptions, that $n_{\text{cr}}/n_i \ll 1$, and that the cosmic ray distribution function can be written as $f(v_\parallel, v_\perp) = f_\parallel(v_\parallel)\, f_\perp(v_\perp)$, then the fluctuation amplitude in mode B_k caused by discrete particle effects can be written as [12, 13],

$$\frac{|B_k|^2}{B_0^2} = \frac{1}{4N_{\text{cr}}\, \Delta T/\Delta t} \frac{\langle v_\perp^2 \rangle_{\text{cr}}^{1/2}}{v_A} f_\parallel\left(\frac{\Omega}{k}\right) \langle v_\perp^2 \rangle^{1/2} \frac{n_{\text{cr}}^2}{n_i^2} \frac{\Omega_i^2}{D_I|_{kv_A}}. \tag{15}$$

We have used N_{cr} as the total number of cosmic rays in the simulation, $\langle v_\perp^2 \rangle \equiv \int f_\perp(v_\perp)\, v_\perp^2\, d^2 v_\perp$, and $D_I|_{kv_A}$ is the imaginary part of the cosmic ray contribution to the dispersion tensor evaluated at $\omega = kv_A$. If $f_\parallel(v_\parallel)$ is symmetric, we can simplify the above expression to

$$\frac{|B_k|^2}{B_0^2} = \frac{1}{8\pi N_{\text{cr}}\, \Delta T/\Delta t} \frac{\langle v_\perp^2 \rangle_{\text{cr}}}{c^2} \frac{\omega_{\text{pcr}}^2}{\Omega_i^2}, \tag{16}$$

at least for the first few modes of the simulation. Test runs with an initially noisy distribution have verified this result to within a factor of three.

As we discussed above, an initially large noise level in the fields will trap the particles and prevent the development of an instability. We would expect this situation to occur when the trapping frequency is of the order of the growth rate Γ. From [14], the trapping frequency in an Alfvén wave is

$$\omega_{\text{trap}} = (kv_\perp \Omega_i)^{1/2} \left(\frac{\tilde{B}_k}{B_0}\right)^{1/2}, \tag{17}$$

where $\tilde{B}$ is the amplitude of the noise field. If the trapping frequency in the noise field is to be less than the growth rate, we must impose a constraint on the number of particles NP and the orbit averaging parameter N, namely,

$$N_{\text{cr}} \cdot \Delta T/\Delta t > \frac{k^2 \langle v_\perp^2 \rangle_{\text{cr}} \omega_{\text{pcr}}^2}{8\pi\Gamma^4} \frac{\langle v_\perp^2 \rangle_{\text{cr}}}{c^2}. \tag{18}$$

In a resonant instability, particles must remain in phase with the wave for a long enough time to exchange energy. In an orbit-averaged code, this criterion means phase information must be maintained throughout each macro-time-step. If the rotation algorithm had no phase error, then θ, the rotation angle for $\mathbf{v} \times \mathbf{B}$ motion in a micro-time-step, would be exactly $\Omega_i \Delta t$. At the conclusion of a macro-time-step, the difference between $\Omega_i \Delta T$ and $N\theta$ must be compared with $\Gamma \Delta T$ to determine whether the resonance condition is significantly shifted. In the limit $\Omega_i \Delta t \ll 0$ we have

$$|\Omega_i \Delta T - N\theta| = N \cdot \frac{(\Omega_i \Delta t)^3}{12} \leqslant \Gamma \Delta T, \tag{19}$$

where Γ is the growth rate of the instability. The corresponding error in $\langle \mathbf{j} \rangle$ and $\langle Q \rangle$ is given by the difference between $P(\Omega_i \Delta t)$ and $P(\theta)$ determined in Eqs. (14b, 20). We have

$$P(\Omega_i \Delta t) - P(\theta) \approx \frac{(\Omega_i \Delta t)^2}{12} + (N+1)\frac{(\Omega_i \Delta t)^4}{24} + O(\Delta t^6). \tag{20}$$

5. Simulations

As a prelude to our study of the full shock-acceleration problem, we have simulated the time evolution of a resonantly unstable distribution of fast, but non-relativistic particles for which a growth rate can be calculated analytically. This problem is a simple way to test the accuracy and stability of our code, and so verify the noise level in the orbit averaging algorithm.

As a simple test of the linear behavior of a single unstable mode, we have adopted a cosmic ray distribution function

$$f(\mathbf{p}) = \frac{\delta(p_\perp)}{4\pi p_\perp} [\delta(p_\parallel - p_0) + \delta(p_\parallel + p_0)] \tag{21}$$

which corresponds to two cold interpenetrating beams. The cosmic ray contribution ray–MHD fluid dispersion relation is

$$\omega^2 - k^2 v_A^2 - \frac{\omega_{\text{pcr}}^2}{2\gamma}\frac{v_A^2}{c^2}\left(\frac{\omega\gamma - kv_0}{\omega\gamma - kv_0 \pm \Omega_i} + \frac{\omega\gamma + kv_0}{\omega\gamma + kv_0 \pm \Omega_i}\right) = 0, \tag{22}$$

where $v_0 = p_0/m$ and γ is the particle Lorentz factor. If we choose computer units such that $\Omega_i = 0.1$, $\omega_{\text{pcr}} = 0.05$, $v_A = 0.01$, $k = 1$, and $c = 1$, then Γ, the imaginary part of the frequency, has a Lorentz profile as a function of beam velocity. The plot of Γ/ω as a function of v_0, shown in Fig. 5, shows that $\Gamma/\omega|_{\max} = 7.85 \times 10^{-2}$ occurs at $v_{\max} = 0.11$, i.e., when the resonance condition

$$\text{Re}(\omega)\gamma \pm kv_0 \pm \Omega_i = 0 \tag{23}$$

is satisfied. A single test run, with 512 particles, an orbit averaging parameter $N = \Delta T/\Delta t = 50$, and a beam velocity $v_0 = 0.11$, gave a measured growth rate $\Gamma/\omega = 7.8 \times 10^{-2}$, in excellent agreement with the above result. We have repeated this run with a slightly different beam velocity, corresponding to $\Gamma/\omega = 4.89 \times 10^{-2}$, and find a measured growth rate of $\Gamma/\omega = 5.0 \times 10^{-2}$. During runs in which the beam energy was 10^{-3} of the total system energy, energy was conserved to better than 10^{-7}, while the momentum was conserved to 0.2% relative to the initial momentum of a cosmic ray. If we were to repeat these simulations without using orbit averaging, we would require 25,000 particles to obtain the same noise level. The approximately 5 Cray-1 CPU min/run would then expand to ~4 h. This example clearly demonstrates the efficacy of our simulation algorithm in studying the supernova remnant acceleration problem.

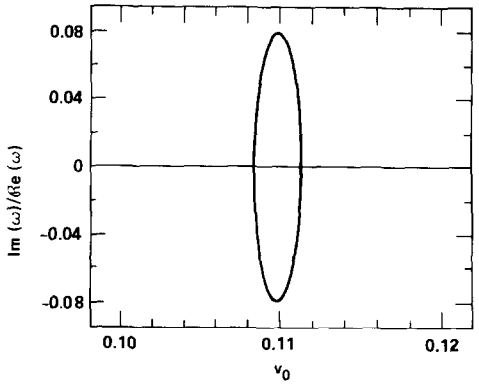

FIG. 5. The ratio of the imaginary part of ω to the real part of ω for two cold interpenetrating beams with a dense MHD background. Using the parameters in the text, this example has a maximum growth rate when $v_0 = 0.11$, i.e., when $\text{Re}(\omega)\gamma - kv_0 \pm \Omega_i = 0$.

ACKNOWLEDGMENTS

We thank J. Arons, R. Freis, D. Hewett, B. Langdon, C. Max, and P. Woodward for their assistance and encouragement. This research was supported under the auspices of the Department of Energy at LLNL under Contract W-7405-ENG-48, and through the Institute of Geophysics and Planetary Physics at LLNL.

REFERENCES

1. G. F. KRYMSKY, *Dokl. Akad. Nauk. SSSR.* **234**, 1306 (1977).
2. W. I. AXFORD, E. LEER, AND G. SKADRON, in *Proc. 15th Int. Cosmic Ray Conf., 1977* (Plovdiv, 1977), Vol. 11, p. 132.
3. A. R. BELL, *Mon. Not. Roy. Astron. Soc.* **182**, 147 (1978); 443.
4. R. D. BLANDFORD AND J. P. OSTRIKER, *Astrophys. J.* **221**, L29 (1978); **237**, 793 (1980).
5. P. O. LAGAGE AND C. J. CESARSKY, *Astron. Astrophys.* **118**, 223 (1983).
6. B. I. COHEN, T. A. BRENGLE, D. B. CONLEY, AND R. P. FREIS, *J. Comput. Phys.* **38**, 45 (1980).
7. B. I. COHEN AND R. P. FREIS, *J. Comput. Phys.* **45**, 367 (1982).
8. A. B. LANGDON AND B. F. LASINSKI, *Methods Comput. Phys.* **16**, 327 (1976).
9. G. A. SOD, *J. Comput. Phys.* **27**, 1 (1978).
10. C. W. HIRT, *J. Comput. Phys.* **2**, 339 (1968).
11. R. C. DAVIDSON, *Methods in Nonlinear Plasma Theory* (Academic Press, New York, 1972), Chap. 4.
12. B. I. COHEN, "Multiple Time Scales," *Computational Techniques* (Academic Press, Orlando, 1985), Chap. 10.
13. C. K. BIRDSALL AND A. B. LANGDON, *Plasma Physics via Computer Simulation* (McGraw–Hill, Hew York, 1985), Chap. 12.
14. N. F. OTANI, *Application of Nonlinear Constants of Motion in a Single Electromagnetic wave to the Study of the Alfven-Ion-Cyclotron Instability*, UCB/ER1 M84/49 (Univ. of California, Berkeley, 1984).